



## Odd-parity superconductors with two-component order parameters: Nematic and chiral, full gap, and Majorana node

Jörn W. F. Venderbos, Vladyslav Kozii, and Liang Fu

*Department of Physics, Massachusetts Institute of Technology, Cambridge, Massachusetts 02139, USA*

(Received 15 December 2015; revised manuscript received 6 March 2016; published 10 November 2016; corrected 22 May 2017)

Motivated by the recent experiment indicating that superconductivity in the doped topological insulator  $\text{Cu}_x\text{Bi}_2\text{Se}_3$  has an odd-parity pairing symmetry with rotational symmetry breaking, we study the general class of odd-parity superconductors with two-component order parameters in trigonal and hexagonal crystal systems. In the presence of strong spin-orbit interaction, we find two possible superconducting phases below  $T_c$ , a time-reversal-breaking (i.e., chiral) phase and an anisotropic (i.e., nematic) phase, and determine their relative energetics from the gap function in momentum space. The nematic superconductor generally has a full quasiparticle gap, whereas the chiral superconductor with a three-dimensional (3D) Fermi surface has point nodes with lifted spin degeneracy, resulting in itinerant Majorana fermions in the bulk and topological Majorana arcs on the surface.

DOI: [10.1103/PhysRevB.94.180504](https://doi.org/10.1103/PhysRevB.94.180504)

**Introduction.** Unconventional superconductors with non- $s$ -wave pairing symmetry have always been an tantalizing topic of condensed matter physics [1]. For inversion-symmetric materials, superconducting order parameters can be broadly divided into two types: even-parity (such as  $s$ -wave) and odd-parity (such as  $p$ -wave). There is mounting evidence that the heavy fermion compound  $\text{UPt}_3$  [2,3] and the transition metal oxide  $\text{Sr}_2\text{RuO}_4$  [4,5] are odd-parity superconductors. In spin-rotational-invariant systems, odd-parity superconductivity generally results from spin-triplet pairing, which can be mediated by spin fluctuations in the vicinity of ferromagnetic instability. On the other hand, the mechanisms and properties of odd-parity superconductivity in spin-orbit-coupled systems have been less explored until recently. In the last few years, a number of theoretical and numerical studies have shown that in the presence of strong spin-orbit interaction, odd-parity pairing can be realized in a broad range of materials without proximity to magnetic instabilities [6–13].

In particular, Fu and Berg [6] proposed that the doped topological insulator  $\text{Cu}_x\text{Bi}_2\text{Se}_3$ , which is superconducting below  $T_c \sim 3.8$  K [14,15] and has strong spin-orbit coupling with a magnitude comparable to the Fermi energy, may have an odd-parity order parameter. This theoretical proposal has sparked considerable experimental studies of  $\text{Cu}_x\text{Bi}_2\text{Se}_3$  and related superconductors derived from topological insulators [16–18]. Remarkably, two recent experimental studies on  $\text{Cu}_x\text{Bi}_2\text{Se}_3$ , both bulk probes of the bulk pairing symmetry, have observed in-plane uniaxial anisotropy appearing below  $T_c$ : Knight shift measurements [19] and specific heat measurements in rotating field [20]. This provides a direct evidence of spontaneous spin rotational symmetry breaking in the superconducting state. Further theoretical analysis [21] shows that this NMR result *and* the absence of line nodes deduced from an earlier specific heat measurement [15] appear to be consistent only with the two-component  $E_u$  order parameter, which is one of the odd-parity pairing symmetries classified in Ref. [6]. Very recent magnetotransport [22] and torque magnetometry [23] measurements further support this.

Motivated by these experimental advances, here we study the physics of odd-parity two-component superconductors.

In general, superconductors with multi-dimensional order parameters may exhibit multiple superconducting phases as a function of temperature, magnetic field, pressure and chemical substitution. These phases may break time-reversal, spin rotation, or crystal symmetry, as exemplified by the  $A$  and  $B$  phases of  $^3\text{He}$ . While time-reversal-breaking (or chiral) superconductivity has been widely studied especially in the context of  $\text{Sr}_2\text{RuO}_4$ , rotational symmetry broken or *nematic* superconductivity, as exhibited by  $\text{Cu}_x\text{Bi}_2\text{Se}_3$ , is however rare and largely unexplored. The main purpose of this work is to study the energetics and physical properties of two-component odd-parity superconductors, and point out the crucial role of spin-orbit coupling.

Our main results are as follows. First, we list the representative gap functions of two-component odd-parity order parameters, which differ significantly for materials with and without spin-orbit interaction. Next, by a weak-coupling analysis based on Bardeen-Cooper-Schrieffer (BCS) theory, we show that in spin-rotational-invariant materials, the energetically favored superconducting phase below  $T_c$  is rotationally invariant, but in the presence of strong spin-orbit coupling, it can be either chiral or nematic. We show that the nematic phase generally has a full superconducting gap, whereas the chiral phase exhibits robust point nodes with *lifted* spin degeneracy on a 3D Fermi surface, resulting in low-energy Majorana-Bogoliubov quasiparticles in the bulk and topological Majorana arcs on the surface.

**Two-component odd-parity order parameters.** Assuming that the superconducting gap is much smaller than the Fermi energy, we construct the superconducting order parameter using electron operators on the Fermi surface:  $\psi(\vec{k}) = [c_1(\vec{k}), c_2(\vec{k})]^T$ . In the absence of spin-orbit coupling the index  $\alpha = 1, 2$  labels two spin eigenstates along a global  $z$  axis. In spin-orbit coupled systems, and in the presence of time-reversal ( $\Theta$ ) and parity ( $P$ ) symmetry,  $\alpha$  is a pseudospin index labeling the two degenerate bands. We choose a special basis, called manifestly covariant Bloch basis (MCBB) [24], in which the  $[c_1, c_2]^T$  obeys the same simple transformation properties under the symmetries of the crystal as an ordinary  $SU(2)$  spinor  $[c_\uparrow, c_\downarrow]^T$  [25].

The pairing potential in BCS mean-field theory of superconductivity can be explicitly expressed in MCBB as  $\hat{\Delta} = \sum_{\vec{k}} \Delta_{\alpha\beta}(\vec{k}) \epsilon_{\beta\gamma} c_{\alpha}^{\dagger}(\vec{k}) c_{\gamma}^{\dagger}(-\vec{k})$ , where the pairing matrix  $\Delta(\vec{k})$  is basis dependent. Time-reversal symmetry acts as  $\Theta \psi(\vec{k}) \Theta^{-1} = i\sigma_y \psi(-\vec{k})$ , and this implies for a time-reversal-invariant pairing function  $(i\sigma_y) \Delta^*(\vec{k}) (-i\sigma_y) = \Delta(-\vec{k})$ . Symmetries of the crystal point group  $G$ , denoted  $g \in G$ , act as  $g \psi(\vec{k}) g^{-1} = U_g \psi(g\vec{k})$ . Odd-parity pairing is then defined by the relation  $\Delta(-\vec{k}) = -\Delta(\vec{k})$ .

The simple transformation properties of the pairing function in the MCBB allow a straightforward classification in terms of representations of the crystal symmetry group. In spin-rotational-invariant systems, the pairing is decomposed into different representations of the symmetry group  $G \times \text{SU}(2)$ . For multicomponent odd-parity superconducting order parameters, the pairing function is a linear combination of the basis functions,  $\Delta(\vec{k}) = \sum_m \xi_m \Delta_m(\vec{k}) \cdot \vec{\sigma}$ , where  $m$  labels the components of the representation, and the order parameters  $\xi_m$  are *vectors* in spin space. Because of the spin-rotational symmetry, superconducting states whose order parameters only differ by a common  $SO(3)$  rotation of all vectors  $\xi_m$  are degenerate in energy. In contrast, in the presence of spin-orbit coupling, the electron spin and momentum transform jointly under crystal symmetry operations. Therefore the pairing function is entirely classified by the symmetry group  $G$ , and  $\Delta(\vec{k})$  is decomposed as  $\Delta(\vec{k}) = \sum_m \eta_m \Delta_m(\vec{k})$ , where  $\eta_m$  are *scalars* and the spin structure is now fixed by  $\Delta_m(\vec{k})$ .

In this work, we consider *two*-component order parameters, i.e.,  $m = 1, 2$ . Then, the pairing functions for spin-rotationally invariant and spin-orbit coupled cases take the form

$$\Delta(\vec{k}) = \vec{\xi}_1 g_1(\vec{k}) \cdot \vec{\sigma} + \vec{\xi}_2 g_2(\vec{k}) \cdot \vec{\sigma}, \quad (1)$$

$$\Delta(\vec{k}) = \eta_1 F_1(\vec{k}) + \eta_2 F_2(\vec{k}), \quad (2)$$

respectively. For example, Table I shows basis functions  $g_{1,2}(\vec{k})$  and  $F_{1,2}(\vec{k})$  in the leading-order  $p$ -wave harmonic expansion for the trigonal  $D_{3d}$  point group of  $\text{Bi}_2\text{Se}_3$ , and the hexagonal  $D_{6h}$  point group of  $\text{UPt}_3$ . Many (but not all) of these basis

TABLE I. Table listing the two-component odd-parity pairings to leading order  $p$  wave in the harmonic expansion. We focus on hexagonal and trigonal crystal systems. The coefficients  $a, b$  multiplying degenerate basis functions are arbitrary, i.e., not determined by symmetry.

Pairing form factors	$D_{3d}$	$D_{6h}$
$g_1(\vec{k}) = k_x$ $g_2(\vec{k}) = k_y$	$E_u$	$E_{1u}$
$F_1^a(\vec{k}) = k_x \sigma_z, F_1^b(\vec{k}) = k_z \sigma_x$ $F_2^a(\vec{k}) = k_y \sigma_z, F_2^b(\vec{k}) = k_z \sigma_y$	$E_u$	$E_{1u}$
$F_1^c(\vec{k}) = k_x \sigma_y + k_y \sigma_x$ $F_2^c(\vec{k}) = k_x \sigma_x - k_y \sigma_y$	$E_u$	$E_{2u}$

functions have been obtained before, see for example Ref. [26] and references therein.

*Landau theory.* To address the phenomenology of odd-parity pairing we consider the Ginzburg-Landau (GL) expansion of the free energy in the order parameter. We first take the spin-orbit coupled case. For the order parameters defined in Eq. (2), the free energy up to fourth order and for all symmetry groups listed in Table I is given by [27,28]

$$F = A(T - T_c)(|\eta_1|^2 + |\eta_2|^2) + B_1(|\eta_1|^2 + |\eta_2|^2)^2 + B_2|\eta_1^* \eta_2 - \eta_1 \eta_2^*|^2. \quad (3)$$

The GL coefficient  $B_2$  decides the superconducting order below  $T_c$  [21,27,28]. When  $B_2 < 0$ , the chiral superconductor, given by  $(\eta_1, \eta_2) = \eta_0(1, \pm i)$ , is favored. Chiral superconductivity, defined by nonzero  $\eta_1^* \eta_2 - \eta_1 \eta_2^*$ , breaks time-reversal symmetry since  $\Theta$  acts  $\eta_i \rightarrow \eta_i^*$ . When  $B_2 > 0$ , the nematic superconductor, given by  $(\eta_1, \eta_2) = \eta_0(\cos \theta, \sin \theta)$ , is favored. The nematic superconductor owes its name to nonzero nematic order  $N_i$  given by  $(N_1, N_2) = (|\eta_1|^2 - |\eta_2|^2, \eta_1^* \eta_2 + \eta_2^* \eta_1)$ . These components satisfy  $N_i^* = N_i$  and therefore are time-reversal invariant. They transform, however, as partners of the  $E_g$  ( $D_{3d}$ ) and  $E_{2g}$  ( $D_{6h}$ ) representations, which implies the nematic superconductor breaks rotational symmetry. The nematic angle  $\theta$  is pinned at three-fold degenerate discrete values only at sixth order in the GL expansion. The term  $F^{(6)} = C_1(N_+^3 + N_-^3)$  with  $N_{\pm} = \eta_1 \pm i\eta_2$  discriminates the two types of nematic states with  $(\eta_1, \eta_2) = \eta_0(1, 0)$  and  $\eta_0(0, 1)$ .

This should be contrasted with the Landau theory for odd-parity triplet pairing in spin-rotational invariant systems, which in terms of  $(\xi_1, \xi_2)$  defined in Eq. (1) is given by, at fourth order,

$$F^{(4)} = B_1(|\xi_1|^2 + |\xi_2|^2)^2 + B_2|\xi_1^* \times \xi_1 + \xi_2^* \times \xi_2|^2 + B_3|\xi_1^* \cdot \xi_2 - \xi_2^* \cdot \xi_1|^2 + B_4(\xi_1^* \times \xi_2 - \xi_2^* \times \xi_1)^2 + B_5(N_1^2 + N_2^2) + B_6(|\vec{N}_1|^2 + |\vec{N}_2|^2), \quad (4)$$

where  $N_{1,2} = \xi_i^a \tau_{ij}^{z,x} \xi_j^a$  and  $N_{1,2}^a = \epsilon^{abc} \xi_i^b \tau_{ij}^{z,x} \xi_j^c$  (repeated indices summed). The GL coefficients  $B_2$ - $B_6$  determine which of the four distinct superconducting states is selected immediately below  $T_c$  [29].

*Weak-coupling energetics below  $T_c$ .* To proceed, we examine the energetics of odd-parity two-component superconductors in weak-coupling BCS theory. In a microscopic theory, the phenomenological GL coefficients can be evaluated as Feynman diagrams, and we exploit the symmetry of the two-component pairings to relate GL coefficients to each other and infer the relative stability of superconducting states [29].

Consider first the triplet superconductors without spin-orbit coupling. For the symmetry groups listed in Table I, using the transformation properties of  $(g_1, g_2)$ , we find that the GL coefficients are related as  $B_1 = B_2 = 2B_5 = 2B_6$  and  $B_3 = B_4 = 0$ . This result is obtained using only the symmetry of the form factors and holds irrespective of the Fermi surface geometry or the form of  $g_{1,2}$  (i.e., order of the harmonic expansion) and leads to a very general conclusion: the rotational-invariant chiral and the helical superconductor are the favored within the weak-coupling analysis, both in 2D

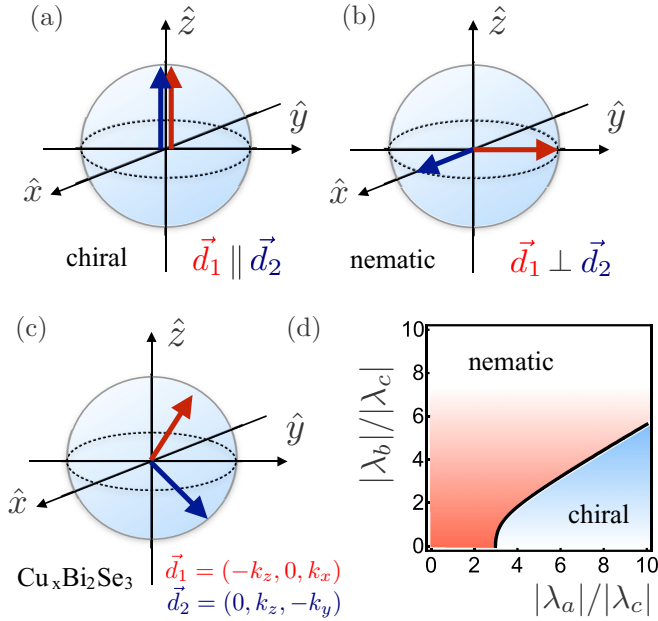


FIG. 1. (a)–(c) Pictorial representation of the geometric criterion for odd-parity two-component superconductors whose  $d$  vectors  $\vec{d}_1(\vec{k})$  and  $\vec{d}_2(\vec{k})$  as function of  $\vec{k}$  are (a) parallel, (b) perpendicular, and (c) have both parallel and perpendicular components. Case (c) applies to the two-orbital model of  $\text{Cu}_x\text{Bi}_2\text{Se}_3$ . (d) Superconducting phase diagram of odd-parity two-component superconductors with hexagonal and trigonal symmetry, obtained for pairings composed of  $F_{1,2}^t(\vec{k})$  with  $t = 1, 2, 3$  and assuming a spherical Fermi surface, in the  $(|\lambda_a|, |\lambda_b|)/|\lambda_c|$  plane.

and 3D, and they remain degenerate at fourth order in GL theory.

Next, we turn to spin-orbit superconductors described by Eq. (3), and study their energetics. We first derive a general expression for the GL coefficients  $B_{1,2}$  and then apply the result to various gap functions given in Table I. We expand the two pairing components of Eq. (2) as  $F_{1,2}(\vec{k}) = \vec{d}_{1,2}(\vec{k}) \cdot \vec{\sigma}$  in terms of real momentum-dependent  $\vec{d}_{1,2}$  vectors (which are locked to the lattice) and calculate the GL coefficients [29]. Remarkably, the result for  $B_2$  can be cast entirely in terms of the  $d$ -vector configuration on the Fermi surface, taking the simple form

$$B_2 = \langle (\vec{d}_1 \times \vec{d}_2)^2 \rangle - \langle (\vec{d}_1 \cdot \vec{d}_2)^2 \rangle, \quad (5)$$

where  $\langle \dots \rangle$  is equal to an average over the Fermi surface. Defining  $I_1 = \langle (\vec{d}_1 \cdot \vec{d}_2)^2 \rangle$  and  $I_2 = \langle (\vec{d}_1 \times \vec{d}_2)^2 \rangle$  we further find  $B_1 = 3I_1 + I_2$ . From this we obtain a general criterion for the superconducting state favored below  $T_c$ : the parallel component  $\vec{d}_1 \parallel \vec{d}_2$  favors the chiral the superconductor whereas the orthogonal component  $\vec{d}_1 \perp \vec{d}_2$  favors the nematic superconductor. A pictorial geometric representation of this is shown in Figs. 1(a)–1(c).

Let us now apply this result to the pairing functions of Table I, and in particular to the case of  $\text{Cu}_x\text{Bi}_2\text{Se}_3$ . For  $E_u$  pairing of  $D_{3d}$  (the point group of  $\text{Cu}_x\text{Bi}_2\text{Se}_3$ ) the gap function is a linear combination of multiple basis functions in the  $p$ -wave harmonic expansion, i.e.,  $F_m(\vec{k}) = \sum_t \lambda_t F_m^t(\vec{k})$  with

$t = a, b, c$  and here the  $\lambda_t$  are not determined by symmetry. The GL coefficients  $B_{1,2}$  will depend on the expansion coefficients  $\lambda_t$  and the details of the Fermi surface [29]. Assuming a three-dimensional Fermi surface, the superconducting phase diagram determined by the sign of  $B_2$  is shown in Fig. 1(d), as a function of  $|\lambda_a|/|\lambda_c|$  and  $|\lambda_b|/|\lambda_c|$ . The location of the material  $\text{Cu}_x\text{Bi}_2\text{Se}_3$  in this phase diagram can be obtained by mapping the two-orbital model [6] to the conduction band MCBB (see Ref. [29]). We find that  $|\lambda_a| \sim |\lambda_b|$  and  $\lambda_c = 0$ . As a result, the nematic superconductor is expected below  $T_c$ , consistent with the observation of rotational symmetry breaking in NMR [19].

In case of  $E_{1u}$  and  $E_{2u}$  pairing in a hexagonal crystal (i.e., symmetry group  $D_{6h}$ ), the gap functions are similarly expanded with expansion coefficients  $\lambda_t$ . Now symmetry forces  $\lambda_c = 0$  ( $E_{1u}$ ) and  $\lambda_a = \lambda_b = 0$  ( $E_{2u}$ ), fixing the location in phase diagram of Fig. 1(d). The nematic superconductor is selected as the lowest energy state independent of the Fermi surface geometry when  $\lambda_a = \lambda_b = 0$ , since parallel component identically vanishes in this case, i.e.,  $\vec{d}_1 \cdot \vec{d}_2 = 0$ .

The appearance of nematic superconductivity in spin-orbit coupled systems should be contrasted with triplet pairing in spin-rotationally invariant superconductors, which always leads to isotropic phases: either chiral or helical. It may also be contrasted with two-component singlet  $d$ -wave superconductors [30] and spinless  $p$ -wave superconductors in 2D [31]: in both cases the isotropic chiral phase ( $p + ip$  and  $d + id$ ) is favored.

*Gap structures.* We now study quasiparticle gap structures of nematic and chiral superconductors with spin-orbit coupling. First, consider the  $E_u$  pairing in trigonal crystals with  $D_{3d}$  point group, whose gap function takes the general form  $\Delta(\vec{k}) = \sum_t \lambda_t (\eta_1 F_1^t(\vec{k}) + \eta_2 F_2^t(\vec{k})) \equiv \vec{d}(\vec{k}) \cdot \vec{\sigma}$ , where  $F_{1,2}^t$  with  $t = a, b, c$  are listed in Table I. A nematic superconductor is obtained when  $\eta_{1,2}$  and  $\lambda_t$  are real. In this case, the superconducting gap is given by  $\delta(\vec{k}) = |\vec{d}(\vec{k})|$ , with  $\vec{k}$  being on the Fermi surface. For generic values of  $(\eta_1, \eta_2)$ , it is vanishingly improbable to find solutions to  $\vec{d}(\vec{k}) = 0$ , which involves *three* independent equations, on the Fermi surface, which is a *two-dimensional* manifold. Therefore, nematic superconductors are generally nodeless [21]. Only for  $\eta_2 = 0$ , a pair of point nodes are present on the  $yz$  plane, and protected by the mirror symmetry  $x \rightarrow -x$ , which remains unbroken in the nematic superconducting state [21].

The quasiparticle gap structures of these nematic superconductors are shown in Figs. 2(a) and 2(b). To make a connection with  $\text{Cu}_x\text{Bi}_2\text{Se}_3$ , we note that experiments have reported a full pairing gap [15], which is consistent with a (0, 1) nematic state. The two-fold anisotropic gap structure of this nematic state provides a direct experimental test of the pairing symmetry of  $\text{Cu}_x\text{Bi}_2\text{Se}_3$ . The normal state Fermi surface has been shown to display doping dependence, becoming open and quasi-2D at high doping [32]. We therefore also plot the quasiparticle gap at  $k_z = 0$  in Fig. 2(c) representative for such case. The difference between open enclosed Fermi surfaces may be a way to reconcile conflicting STM measurement studies [33,34].

Hexagonal crystals have higher symmetry and therefore potentially more constraints on the gap structure. In particular,

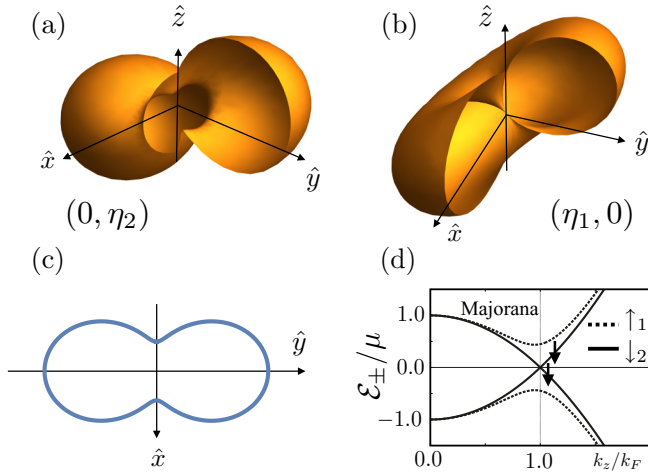


FIG. 2. (a)–(b) Quasiparticle gap structures of odd-parity superconductors with  $(0,1)$  and  $(1,0)$  nematic components, showing the absence and presence of nodes, respectively. (c) Quasiparticle gap of  $(0,1)$  nematic superconductor as function of azimuthal angle for  $k_z = 0$ . (d) Quasiparticle spectrum  $\mathcal{E}_\pm$  along  $k_z$  of chiral superconductor  $(1,i)$  showing Majorana node.

certain gap function coefficients  $\lambda_i$  are forced to vanish in certain pairing channels. In case of  $E_{1u}$  pairing, all nematic superconductors have a pair of point nodes in the  $xy$  plane due to a mirror symmetry  $z \rightarrow -z$ . In case of  $E_{2u}$  pairing, the gap function  $\Delta(\vec{k})$  vanishes on the  $z$  axis, resulting in a pair of point nodes on a 3D Fermi surface. However, for generic values of  $(\eta_1, \eta_2)$ , the nematic superconductor with lowered crystal symmetry allows a small admixture of a new gap function  $F_{A_{1u}}(\vec{k}) = k_z \sigma_z$ , whose presence leads again to a full superconducting gap. Only for special cases of  $(\eta_1, \eta_2) = (\cos \theta_0, \sin \theta_0)$  with  $\theta_0 = (n + 1/2)\pi/3$ , the presence of two mirror symmetries  $x \rightarrow -x$  and  $y \rightarrow -y$  protect the nodes along the  $z$  axis. We have thus shown that nematic superconductors with odd-parity order parameters generally have a full gap, except for special cases associated with the presence of a mirror symmetry [29].

In contrast, chiral superconductors with complex  $\vec{d}$  vector  $(\eta_1, \eta_2) = (1, \pm i)$  have a different gap structure. Of particular interest is the chiral superconductor with the  $D_{3d}$  point group and  $E_u$  pairing. From the gap function, we find this pairing yields a nonunitary state with different gaps for the two pseudospin species. On a 3D Fermi surface, a particular pseudospin species determined by the chirality of the order parameter,  $\sigma_z = -1(1)$  for the case of  $\eta_2/\eta_1 = i(-i)$ , is gapless on the north and south poles  $\pm \vec{K} = (0, 0, \pm k_F)$ , whereas the other spin species has a full gap, which is proportional to  $\lambda_b$  at  $\pm \vec{K}$ . This leads to a rare case of point nodes *without* spin degeneracy. As a result, the Bogoliubov quasiparticles near these two nodes form a *single* flavor of massless Majorana fermions in three dimensions as in particle physics. They are described by a *four-component, real* quantum field  $\Psi(\vec{x})$ , consisting of electron fields of a spin component near  $\vec{K}$ :

$$\Psi^\dagger(x) = \sum_{\vec{q}} e^{i\vec{q}\cdot\vec{x}} (c_{\vec{K}+\vec{q}}^\dagger, c_{-\vec{K}+\vec{q}}^\dagger, c_{\vec{K}-\vec{q}}, c_{-\vec{K}-\vec{q}}). \quad (6)$$

Importantly, the field  $\Psi$  lives in Nambu space and satisfies the reality condition of Majorana fermions,  $\Psi^\dagger(\vec{x}) = (\tau_x \Psi(\vec{x}))^T$ . The low-energy Hamiltonian for these Majorana-Bogoliubov quasiparticles, in case of  $\eta_2/\eta_1 = i$ , is given by

$$H_+ = \frac{1}{2} \sum_{\vec{q}} \Psi_{\vec{q}}^\dagger \begin{pmatrix} v_F q_z & 0 & 0 & v_\Delta i q_- \\ 0 & -v_F q_z & v_\Delta i q_- & 0 \\ 0 & -v_\Delta i q_+ & v_F q_z & 0 \\ -v_\Delta i q_+ & 0 & 0 & -v_F q_z \end{pmatrix} \Psi_{\vec{q}}, \quad (7)$$

where  $q_\pm = q_x \pm i q_y$ ,  $v_F$  is Fermi velocity in the  $z$  direction, and  $v_\Delta = 2\eta_0 \lambda_c$  with pairing amplitude  $\eta_0$ . The Hamiltonian  $H_-$  for the opposite chirality  $\eta_2/\eta_1 = -i$  is obtained by interchanging  $q_+$  and  $q_-$ . The quasiparticle dispersion near the nodes is linear in all directions, as shown in Fig. 2(d). The presence of gapless Majorana fermions is a unique feature of chiral superconductors with spin-orbit coupling and 3D Fermi surface [35]. It should be contrasted with either the nematic superconductor or  $p_x \pm i p_y$  superfluid  $^3\text{He}$ , both of which have *spin-degenerate* point nodes giving rise to a four-component Dirac fermions instead of Majorana. Moreover, the chiral superconductor with  $E_u$  pairing becomes fully gapped when the Fermi surface topology changes from a closed pocket to an open cylinder [32].

The gap structures of both nematic and chiral superconductors, including the gap anisotropy and nodal quasiparticles, can be detected by tunneling, specific heat and thermal conductivity under a rotating field, as well as temperature- and angle-dependent London penetration depth. The chiral superconductor is topological and has chiral Majorana fermion surface states. When the bulk has point nodes, zero-energy surface states form a *single* open arc in two-dimensional momentum space, connecting the projection of the nodes. Importantly, this Majorana arcs has half degrees of freedom as surface arcs in Weyl semimetals [36] or superconductors with spin-degenerate nodes [37–40]. When the bulk is fully gapped, surface states consist of an array of one-dimensional chiral Majorana fermions stacked along the  $z$  axis. The presence of chiral Majorana fermions on the surface gives rise to a topological thermal Hall effect, which we will study in detail elsewhere.

To summarize, odd-parity superconductivity with two-component order parameters in spin-orbit-coupled materials comes in two flavors: nematic and chiral. The relative energetics of these two phases is determined by the spin texture of the gap function, i.e., the geometry of  $d$  vectors over the Fermi surface, as shown in Eq. (5). The gap structures of nematic and chiral phases are obtained, and nodal quasiparticles in the latter case are identified as undoubled 3D Majorana fermions. Our results directly apply to a number of materials currently receiving much attention, including  $\text{Cu}_x\text{Bi}_2\text{Se}_3$  and possibly  $\text{Sr}_x\text{Bi}_2\text{Se}_3$  [16] and  $\text{Nb}_x\text{Bi}_2\text{Se}_3$  [41].

*Acknowledgment.* We thank Yoichi Ando and Yew San Hor for discussions. This work is supported by DOE Office of Basic Energy Sciences, Division of Materials Sciences and Engineering under Award No. DE-SC0010526. L.F. is supported partly by the David and Lucile Packard Foundation. J.V. is supported by the Netherlands Organization for Scientific Research (NWO) through a Rubicon grant.

- [1] M. R. Norman, *Science* **332**, 196 (2011).
- [2] J. A. Sauls, *Adv. Phys.* **43**, 113 (1994).
- [3] R. Joynt and L. Taillefer, *Rev. Mod. Phys.* **74**, 235 (2002).
- [4] T. M. Rice and M. Sigrist, *J. Phys.: Condens. Matter* **7**, L643 (1995).
- [5] A. Mackenzie and Y. Maeno, *Rev. Mod. Phys.* **75**, 657 (2003).
- [6] L. Fu and E. Berg, *Phys. Rev. Lett.* **105**, 097001 (2010).
- [7] S. Nakosai, Y. Tanaka, and N. Nagaosa, *Phys. Rev. Lett.* **108**, 147003 (2012).
- [8] X. Wan and S. Y. Savrasov, *Nat. Commun.* **5**, 4144 (2014).
- [9] P. M. R. Brydon, S. Das Sarma, H.-Y. Hui, and J. D. Sau, *Phys. Rev. B* **90**, 184512 (2014).
- [10] P. Hosur, X. Dai, Z. Fang, and X.-L. Qi, *Phys. Rev. B* **90**, 045130 (2014).
- [11] T. Yoshida, M. Sigrist, and Y. Yanase, *Phys. Rev. Lett.* **115**, 027001 (2015).
- [12] V. Kozii and L. Fu, *Phys. Rev. Lett.* **115**, 207002 (2015).
- [13] Y. Ando and L. Fu, *Ann. Rev. Condens. Mater. Phys.* **6**, 361 (2015).
- [14] Y. S. Hor, A. J. Williams, J. G. Checkelsky, P. Roushan, J. Seo, Q. Xu, H. W. Zandbergen, A. Yazdani, N. P. Ong, and R. J. Cava, *Phys. Rev. Lett.* **104**, 057001 (2010).
- [15] M. Kriener, Kouji Segawa, Zhi Ren, Satoshi Sasaki, and Yoichi Ando, *Phys. Rev. Lett.* **106**, 127004 (2011).
- [16] Zhongheng Liu, Xiong Yao, Jifeng Shao, Ming Zuo, Li Pi, Shun Tan, Changjin Zhang, Yuheng Zhang, *J. Am. Chem. Soc.* **137**, 10512 (2015).
- [17] Shruti, V. K. Maurya, P. Neha, P. Srivastava, and S. Patnaik, *Phys. Rev. B* **92**, 020506(R) (2015).
- [18] Satoshi Sasaki, Kouji Segawa, and Yoichi Ando, *Phys. Rev. B* **90**, 220504(R) (2014).
- [19] K. Matano, M. Kriener, K. Segawa, Y. Ando, and Guo-qing Zheng, *Nat. Phys.* **12**, 852 (2016).
- [20] S. Yonezawa, K. Tajiri, S. Nakata, Y. Nagai, Z. Wang, K. Segawa, Y. Ando, and Y. Maeno, *Nature Phys.* (2016).
- [21] L. Fu, *Phys. Rev. B* **90**, 100509(R) (2014).
- [22] Y. Pan, A. M. Nikitin, G. K. Araizi, Y. K. Huang, Y. Matsushita, T. Naka, and A. de Visser, *Sci. Rep.* **6**, 28632 (2016).
- [23] T. Asaba, B. J. Lawson, C. Tinsman, L. Chen, P. Corbae, G. Li, Y. Qiu, Y. S. Hor, L. Fu, and L. Li, [arXiv:1603.04040](https://arxiv.org/abs/1603.04040).
- [24] L. Fu, *Phys. Rev. Lett.* **115**, 026401 (2015).
- [25] If spin-orbit interaction is adiabatically switched off, the MCBB smoothly evolve into spin eigenstates, i.e.,  $c_1 \rightarrow c_\uparrow$  and  $c_2 \rightarrow c_\downarrow$ .
- [26] S. K. Yip, *Phys. Rev. B* **87**, 104505 (2013).
- [27] M. Sigrist and K. Ueda, *Rev. Mod. Phys.* **63**, 239 (1991).
- [28] G. E. Volovik and L. Gork'ov, *Sov. Phys. JETP* **61**, 843 (1985).
- [29] See Supplemental Material at <http://link.aps.org/supplemental/10.1103/PhysRevB.94.180504> for details of the analysis of Ginzburg-Landau theories and quasiparticle gap structures. An explicit mapping from the orbital basis of the  $\text{Cu}_x\text{Bi}_2\text{Se}_3$  model Hamiltonian to the MCBB is also provided.
- [30] R. Nandkishore, A. V. Chubukov, and L. Levitov, *Nat. Phys.* **8**, 158 (2012).
- [31] M. Cheng, K. Sun, V. Galitski, and S. Das Sarma, *Phys. Rev. B* **81**, 024504 (2010).
- [32] E. Lahoud, E. Maniv, M. S. Petrushevsky, M. Naamneh, A. Ribak, S. Wiedmann, L. Petaccia, Z. Salman, K. B. Chashka, Y. Dagan, and A. Kanigel, *Phys. Rev. B* **88**, 195107 (2013).
- [33] S. Sasaki, M. Kriener, K. Segawa, K. Yada, Y. Tanaka, M. Sato, and Y. Ando, *Phys. Rev. Lett.* **107**, 217001 (2011).
- [34] N. Levy, T. Zhang, J. Ha, F. Sharifi, A. A. Talin, Y. Kuk, and J. A. Stroscio, *Phys. Rev. Lett.* **110**, 117001 (2013).
- [35] A comprehensive study of Majorana nodes in chiral spin-orbit coupled superconductors will be presented elsewhere; see V. Kozii, J. W. F. Venderbos, and L. Fu, [arXiv:1607.08243](https://arxiv.org/abs/1607.08243).
- [36] Xiangang Wan, Ari M. Turner, Ashvin Vishwanath, and Sergey Y. Savrasov, *Phys. Rev. B* **83**, 205101 (2011).
- [37] G. E. Volovik, *The Universe in a Helium Droplet* (Oxford University Press, Oxford, 2003).
- [38] T. Meng and L. Balents, *Phys. Rev. B* **86**, 054504 (2012).
- [39] J. D. Sau and S. Tewari, *Phys. Rev. B* **86**, 104509 (2012).
- [40] Shengyuan A. Yang, Hui Pan, and Fan Zhang, *Phys. Rev. Lett.* **113**, 046401 (2014).
- [41] Y. Qiu, K. N. Sanders, J. Dai, J. E. Medvedeva, W. Wu, P. Ghaemi, T. Vojta, and Y. S. Hor, [arXiv:1512.03519](https://arxiv.org/abs/1512.03519).